Diode-side-pumped Nd:$YLiF_4$ laser emitting at 1053 nm with 53.6% optical efficiency and diffraction-limited beam quality

2013 Laser Phys. Lett. 10 035807

(http://iopscience.iop.org/1612-202X/10/3/035807)

Laser Phys. Lett. **10** (2013) 035807 (5pp) doi:10.1088/1612-2011/10/3/035807

LETTER

Diode-side-pumped Nd:$YLiF_4$ laser emitting at 1053 nm with 53.6% optical efficiency and diffraction-limited beam quality

Niklaus U Wetter[1] **and Alessandro M Deana**[2]

[1] Instituto de Pesquisas Energéticas e Nucleares, CNEN-IPEN/SP, São Paulo, Brazil
[2] Universidade Nove de Julho, Uninove, São Paulo, Brazil

E-mail: nuwetter@ipen.br

Received 6 June 2012
Accepted for publication 8 November 2012
Published 5 February 2013
Online at stacks.iop.org/LPL/10/035807

Abstract
We present a Nd:$YLiF_4$ diode-side-pumped resonator architecture based on a gain-guided, mode-selective technique that employs a double pass of the fundamental laser mode through the crystal. The folded cavity is very compact, robust and cost efficient. With this design we demonstrate 19 W of quasi-cw, stable diffraction-limited laser emission at 1053 nm when pumping at 792 nm with 35.4 W. The slope efficiency of the laser is 65.3% and the optical-to-optical efficiency is 53.6%, which is, to the best of our knowledge, the highest efficiency reported for Nd:$YLiF_4$ lasers pumped into the $^4F_{5/2}$ band, including longitudinal pumping schemes and lasers emitting at the higher gain line of 1047 nm.

(Some figures may appear in colour only in the online journal)

1. Introduction

In the past few years, a large effort has been made by the academic community aiming at the development of new laser sources capable of providing diffraction-limited beam quality, high power and high efficiency at reduced cost and complexity [1–3].

The development of novel diode-pumped solid-state laser (DPSSL) resonators emitting in the 1 μm region is a major field of research pushed by industrial applications, where the DPSSL has become the number one selling laser design followed by high power fibre lasers. Recently, the laser market increased to US $7.5 billion with the industrial laser market share representing 40% of this total [4].

High pulse energy laser oscillation can be achieved by employing a lamp-pumped design, but this technology is limited to repetition rates of tens of hertz and generally suffers from poor beam quality and very low efficiency [5].

High power laser diodes (or simply diode bars) allow for good overlap of the pump energy and the fundamental laser mode due to their inherent directional emission, therefore favouring the TEM_{00} laser mode with good efficiency. Additionally, they can easily produce kilohertz-level repetition rates.

Several host materials have been tested aiming at efficient laser operation in this region [6–10]. Among them, the $YLiF_4$ (YLF) matrix has a very interesting laser line at 1053 nm that matches the emission wavelength of neodymium-doped glass amplifiers, and also the sum frequency of this transition with the 1338 nm emission from the Nd:YAG laser matches the sodium D2 absorption line [11, 12].

Besides its wavelength, the Nd:YLF gain medium shows some interesting features, such as natural birefringence and

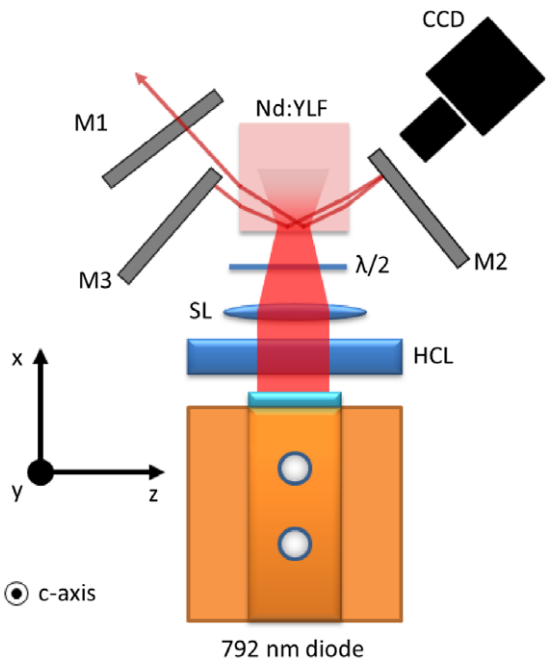

Figure 1. Schematic diagram of the laser cavity setup. M1, M3 are plane mirrors and M2 is a concave folding mirror. Focusing of the pump is achieved by a cylindrical lens (HCL) and a spherical lens (SL). A CCD camera behind the folding mirror measures the transverse beam mode as well as beam separation D.

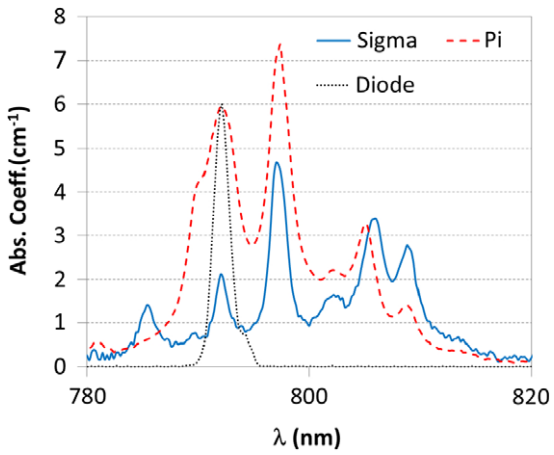

Figure 2. Absorption coefficient of the 1 mol% Nd:YLF and diode emission. Pump polarization is in the crystal's π-direction.

weak thermal lensing that occurs in consequence of the negative refractive index shift with increasing temperature together with the positive lens originating from the thermally induced stress [13, 14]. The long upper laser level lifetime of this active medium permits good energy storage capabilities, allowing us to efficiently operate under Q-switching [15–17].

Although there are many different cavity geometries for DPSSL, they can be divided into two main categories: longitudinal-pumped and side-pumped resonators [18, 19, 7].

With today's high power fibre-coupled diodes, the pump beam can be configured to match the fundamental mode of an end-pumped resonator, thereby allowing good beam quality and high efficiency. On the other hand, end-pumping is usually limited to two pump sites—one on each end of the gain media—and therefore limited in terms of power scaling. In such a configuration, the low fracture limit of the YLF matrix is easily surpassed and care must be taken in order to avoid fracture of the active medium [20]. The highest optical efficiency reported so far for this host was achieved by extracting 1 W of output power at 1047 nm (which has a higher emission cross section than the 1053 nm transition) by end-pumping the crystal with 2 W at 806 nm from a Ti:sapphire laser, which is known for its narrow emission. This corresponds to an optical-to-optical efficiency of 50% (55.6% slope efficiency) [21].

The side-pumping scheme generally employs a lower pump power density and permits power scaling; however, this usually occurs at the expense of the beam quality and efficiency. Stable TEM_{00} emission at 1053 nm with 48% optical-to-optical efficiency (61% slope efficiency) corresponding to 16.7 W peak output power has been obtained for a quasi-continuous (qcw) laser that was optimized for Q-switching operation [22].

In this letter we report a side-pumped resonator architecture based on a folded double pass resonator design employing a square Nd:YLF active crystal, that is capable of delivering tens of watts of stable TEM_{00} output power without the need to introduce any loss-based mode selection technique, thereby achieving record efficiency.

2. Experimental setup

Figure 1 shows a schematic diagram of our laser architecture. The pump source is a qcw diode bar with peak emission at 792 nm when operated at 27°C with a duty cycle below 8%. Its spectral bandwidth is 2 nm FWHM and we verified that its spectrum consists of one single peak. This is important because of the narrow spectral absorption features of Nd:YLF. The 797 nm absorption peak of our crystal is higher than the 792 nm peak, but it is also narrower, as shown in figure 2. A diode of 2 nm bandwidth would cause a poorer overlap at 797 nm, thereby resulting in lower efficiency, as was experimentally verified with our setup. However, our simulations show that it would be advantageous, in terms of efficiency, to pump at the 797 nm absorption peak if the diode had a spectral bandwidth narrower than 0.5 nm FWHM.

The 40 W, TM-polarized and fast-axis collimated diode was focused into the crystal by an $f = 25$ mm spherical lens (SL) and an $f = 25$ mm horizontal cylindrical lens (HCL), resulting in a spot size of approximately 4 mm width and 0.1 mm height (horizontal and vertical directions in figure 1). A half wave plate was employed to rotate the diode's polarization by 90° in order to access the crystal's highly absorbing π-polarization. After the focusing optics and Fresnel reflection at the uncoated pump facet, about 88.5% of the pump power was effectively absorbed by the slab.

The active medium contains nominally 1 mol% neodymium doping level at the yttrium site. The Nd:YLF sample is $13 \times 13 \times 3$ mm^3 in dimension and was a-cut with its c-axis orientated parallel to the y axis as shown in figure 1.

M2 is a curved highly reflective folding mirror with 3 m radius of curvature (ROC) placed as close as possible to the slab's facet. The largest beam waist inside this resonator setup is near the curved folding mirror M2. The two beams enter and exit the crystal at the Brewster angle and undergo total internal reflection at the pump facet.

M1 is a plane output coupler, for which we tested transmissions ranging from 5% to 70% at 1053 nm, and M3 is a flat high reflectivity (HR) mirror. Since M2 has a long ROC, and the active medium does not present any significant thermal lens, this resonator shows stable operation for a wide range of distances between the active medium and both plane mirrors (M1 and M3), varying from a few to tens of centimetres.

For a gain crystal with high absorption cross section, such as Nd: YVO_4 or Nd:$GdVO_4$, a single grazing incidence total internal reflection at the pump surface allows for good overlap between the inverted gain region and the fundamental resonator mode [10]. But for Nd:YLF, which has a lower absorption coefficient (figure 2), a single pass through the gain media would result in multimode operation, as has been demonstrated in previous work [23].

By inserting an additional mirror (M2), a second pass through the gain medium is introduced, resulting in a total of two internal reflections at the pump surface, improving thereby the overlap between the pump beam and the lowest order resonator mode [24].

In this laser design, the two beams, that are almost parallel within the gain crystal and laterally offset in the pump direction (x-axis direction), compete with each other for gain. Therefore, the maximum pump power at which the laser still oscillates with TEM_{00} beam quality is first calculated and simulated as a function of the separation and dimension of both beams, and then adjusted experimentally [22, 24, 25].

3. Simulations

Aiming high efficiency and output power, the resonator configuration was simulated and optimized in terms of resonator geometry, diode characteristics, crystal shape and doping level, using a space dependent MATLAB code, which was developed using a theoretical model based on [26]. This code calculates the output power and the threshold of higher order transversal modes, as a function of overlap between spatial population inversion and laser mode distribution according to the following equation:

$$\int_{\text{cavity}} \frac{s_i r}{1 + \sum_j S_j s_j / I_s} \mathrm{d}V = \frac{I_s \gamma_i}{R}. \qquad (1)$$

Here i represents the index of the new mode that enters laser oscillation when the other j modes are already oscillating, S is the total photon number of the mode, s and r are the normalized distribution functions of the lasing modes and the pump radiation, respectively, I_s is the photon saturation density, γ is the cavity decay time and R is the pump photon flux [23].

The software calculates the pump threshold at which a higher order mode starts to oscillate, as a function of the cavity parameters, after the fundamental mode has already initiated its oscillation. It is a particular feature of this type of side-pumped cavity that it initiates oscillation always in TEM_{00} mode, as has been shown in [24]. Cavity parameters are then adjusted in order to extend the pump power range at which TEM_{00} mode oscillation occurs until either the required output power is obtained or the diode's pump power limit is reached. This is mainly achieved by changing the intra-cavity beam geometry: the separation of the two beams inside the crystal D and the beam radius w. In the next step, an optimization procedure is commenced with the objective to achieve the highest possible optical-to-optical efficiency. Amongst the many parameters that can be influenced are pump spot size, pump wavelength and neodymium doping level.

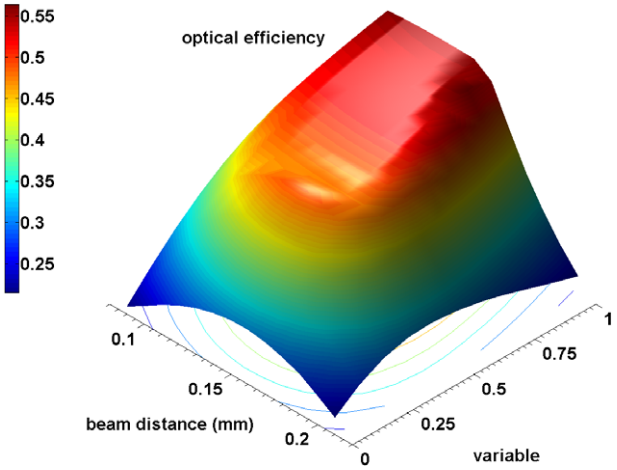

Figure 3. Simulation of the efficiency as a function of D and a generic variable. var = 0 represents the experimental conditions of our earlier work [24] and var = 1 the experimental and spectroscopic parameters described in this work.

After having thoroughly simulated this cavity using our previous results as the basis, we came to the conclusion that only an increase in neodymium doping concentration would lead to considerably better results in terms of qcw efficiency, as required for the passively Q-switched resonator [24, 22, 25].

Figure 3 shows a simulation of the lasers' efficiency as a function of beam separation D and a generic variable var. As this variable changes from 0 to 1 the laser parameters change gradually from our previous results [24] to the results presented in this work: the output coupler changes from 10% transmission to 20%, the width of the pump beam changes from 4.4 to 4 mm and the crystal absorption coefficient changes from 2.8 to 6 cm^{-1} (see figure 2). For the simulations we used losses of 2%, a total cavity length of 40 cm and standard spectroscopic parameters as given in [27]. The two simulated curves in figure 4 correspond to the position of var = 0 and 1 in figure 3.

4. Results

The separation D between the two beams inside the crystal was varied in order to determine for which set of pump powers and separations D the laser oscillates at diffraction limited

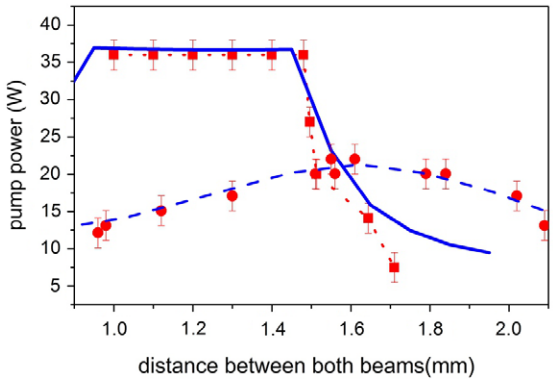

Figure 4. Pump power threshold at which the laser mode changes from TEM_{00} to TEM_{10} as a function of the separation D between the two beams inside the crystal. Solid line and squares: simulation and results, respectively, obtained for the results presented in this work. Dashed line and dots: simulation and results, respectively, obtained primarily with lower doping levels (presented in [23, 24]). Error bars represent the standard deviation of the measurement.

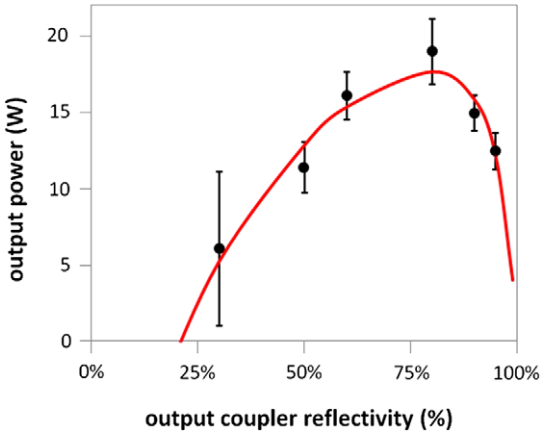

Figure 5. Output power as a function of the output coupler reflectivity for a pump power of 35 W. The solid line represents a theoretical model for a four-level laser system [5].

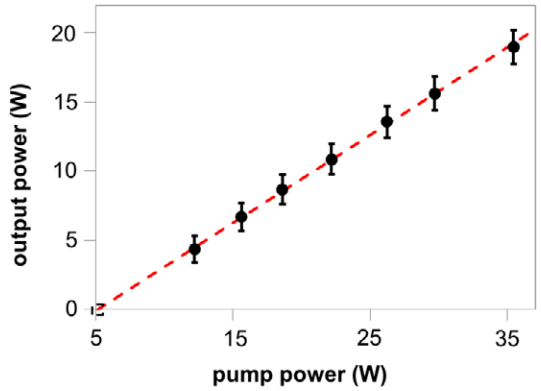

Figure 6. Output power versus pump power of the resonator using an output coupler of 20% transmission.

beam quality. The experimental data of figure 4 were obtained by gradually increasing the pump power at a fixed separation D between the two beams while monitoring the beam quality with a CCD camera placed 3 cm behind mirror M2 in figure 1.

The first mode to oscillate is the TEM_{00}, followed by a higher order, which is not necessarily the next higher order mode TEM_{10} [24]. Figure 4 shows that pure TEM_{00} oscillation is obtainable for a separation D ranging from approximately 1 to 1.5 mm at maximum pump power, and therefore does not require critical adjustment.

Increasing the pump power while maintaining TEM_{00} operation is possible by two means, as shown in [24]: generating a larger beam waist or increasing the effective absorption cross section. In this work, better efficiency was achieved, in comparison with our previously reported results, by using crystals with a higher neodymium doping concentration, therefore increasing the effective absorption [23]. The output coupler transparency was also optimized for qcw operation, as opposed to the Q-switch regime of our previous work [22]. The higher absorption and the correct adjustment of D allows for a very efficient screening of the inverted population by the double pass configuration of the fundamental mode through the active media, resulting in higher order modes to find insufficient gain to overcome the resonator losses without the need for introducing other mode-selective techniques.

Due to the low fracture limit of the YLF host, cw operation was used only up to 10 W of input power. Beyond this input power, qcw operation was employed, permitting high pump powers without the risk of fracturing the crystal. Although in this work we limited the repetition rate to 71 Hz and pump pulse duration to 1 ms, higher repetition rates, up to 1 kHz, have already been demonstrated for this setup [25]. The duty cycle was 7.1%. Furthermore, no particular care was taken in terms of refrigerating the gain crystal, which was placed on top of a copper block using thermal grease.

The whole layout of this cavity is optimized to generate efficiently high power short Q-switched pulses taking full advantage of the crystal's long upper state life time of 520 μs, but it is also capable of delivering high power and efficiency at qcw conditions. Additionally, this cavity is extremely robust and does not need coatings due to Brewster angle incidence, which makes it suited for high power fundamental mode Q-switching.

The laser output power was measured using different output couplers with transmissions ranging from 5% to 70%, as shown in figure 5. For each output coupler, the optical-to-optical power conversion efficiency η_{opt} was measured. η_{opt} incorporates the $\lambda_{laser}/\lambda_{pump}$ ratio, which, in our case, is 1.33. We corrected the η_{opt} by this factor and inferred the photon-to-photon conversion efficiency η in order to perform Caird's loss and pumping efficiency analysis [28]. By employing this analysis, we obtained a pumping efficiency of $\eta_p = 0.66 \pm 0.17$ and cavity losses of $L = 2.0\% \pm 0.4\%$. The analysis is in good agreement with the results of the simulation obtained in figure 4. Considering the available pump power and our resonator architecture, the output laser power is maximized if an output coupler with 20% transmission at 1053 nm is employed, as shown in figure 5.

The slope efficiency and laser threshold obtained with this configuration can be seen in figure 6.

The laser threshold was 5.1 W and the overall power fluctuation, after a few minutes of warm-up time, was less than $\leq$2% over a test period of 4 h (limited by detector precision).

From figure 6 we obtain a slope efficiency of 63.5%. At 35.4 W of absorbed power, the laser delivers 19 W peak power with diffraction limited beam quality ($M^2 = 1.31$), resulting in an optical-to-optical efficiency of 53.6% which is, to the best of our knowledge, the highest efficiency obtained with $^4F_{5/2}$-band pumping (800 nm band) reported for the $^4F_{3/2} \rightarrow {}^4I_{11/2}$Nd:YLF$_4$ main laser transition, considering both polarizations (π and σ) and both geometries (side and end pumped).

In theory, even higher efficiencies could be obtained while maintaining TEM$_{00}$ beam quality by increasing the effective absorption of the pump beam; however, in this case one should also account for the increasing up-conversion and scattering losses.

5. Conclusions

In conclusion, we have demonstrated that our cavity architecture is capable of delivering tens of watts of peak power in qcw operation with diffraction limited beam quality. By correctly modelling the resonator parameters we achieve an optimized laser setup that results in 53.6% optical-to-optical efficiency, which is, to the best of our knowledge, the highest efficiency ever reported for a 800 nm band pumped Nd:YLF laser emitting in the 1 μm region, including end-pumped laser designs.

Acknowledgments

The authors would like to thank FAPESP and CNPq for the financial support of this work.

References

[1] Chen F, Liu J, Wang W W, Fan X W and Quin L J 2009 *Laser Phys. Lett.* **6** 441–4
[2] Zhang S, Yang J F, Xu J L and Yang X Q 2009 *Laser Phys. Lett.* **6** 571–4
[3] Liu H, Gong M, Wushouer X and Gao S 2010 *Laser Phys. Lett.* **7** 124–9
[4] Savage N 2012 *Nature Photon.* **6** 215–6
[5] Koechner W 2006 *Solid-State Laser Engineering: A Graduate Text* (*Springer Series in Optical Sciences*) (Berlin: Springer) p 409
[6] Yang J, Liu J and He J 2005 *Laser Phys. Lett.* **2** 171–3
[7] Zhao S, Huang H T, He J L, Zhang B T, Yang J F, Xu J L and Yang X Q 2009 *Laser Phys. Lett.* **6** 571–4
[8] Kang H X, Zhang H, Yan P, Wang D S and Gong M 2008 *Laser Phys. Lett.* **5** 879–81
[9] Shan C X, Li J, Zhao B and Chen J Z 2010 *Laser Phys. Lett.* **7** 116–9
[10] Danzen M J, Trew M, Rosas E and Crofts G J 2001 *Opt. Commun.* **196** 237–41
[11] Kelly J H *et al* 2006 *J. Phys.* IV **133** 75–80
[12] Zhao Z M, Gao X and Lin J Q 2010 *Laser Phys. Lett.* **7** 719–21
[13] Cerullo G, Desilvestri S and Magni V 1992 *Opt. Commun.* **93** 77–81
[14] Vanherzeele H 1988 *Opt. Lett.* **13** 369–71
[15] Sun Y, Zhang H, Liu Q, Huang L, Wang Y and Gong M 2010 *Laser Phys. Lett.* **7** 722–5
[16] Pati B, Wall K F, Isaynova Y and Moulton P F 2008 *Conf. on Lasers and Electro-Optics & Quantum Electronics and Laser Science Conf.* vol 1–9 pp 120–1
[17] Deana A M, Sousa E C, Ranieri I M, Baldochi S L and Wetter N U 2012 *Appl. Phys.* B **106** 877–80
[18] Yan X, Liu Q, Huang L, Wang Y, Huang X, Wang D and Gong M 2008 *Laser Phys. Lett.* **5** 185–8
[19] Lyashedko A D, Seregin V F, Shcherbakov I A and Tsvetkov V B 2012 *Laser Phys. Lett.* **9** 340–3
[20] Bernhardi E H, Forbes A, Bollig C and Esser M J D 2008 *Opt. Express* **16** 11115–23
[21] Lue Y F, Zhang X H, Zhang A F, Yin X D and Xia J 2010 *Opt. Commun.* **283** 1877–9
[22] Deana A M and Wetter N U 2012 *Proc. SPIE* **8433** 84330B
[23] Wetter N U, Sousa E C, Camargo F A, Ranieri I M and Baldochi S L 2008 *J. Opt. A: Pure Appl. Opt.* **10** 104013
[24] Wetter N U, Sousa E C, Ranieri I M and Baldochi S L 2009 *Opt. Lett.* **34** 292–4
[25] Deana A M, Sousa E C, Ranieri I M, Baldochi S L and Wetter N U 2012 *Proc. SPIE* **8235** 82350G
[26] Kubodera K and Otsuka K 1979 *J. Appl. Phys.* **50** 653–9
[27] Pollnau M, Hardman P J, Kern M A, Clarkson W A and Hanna D C 1998 *Phys. Rev.* B **58** 16076–92
[28] Caird J, Payne S, Staver P, Ramponi A, Chase L and Krupke W 1988 *IEEE J. Quantum Electron.* **24** 1077–99